International Review of Electrical Engineering (I.R.E.E.), Vol. 2, N. 4
July – August 2007

Single-Phase Unity Power Factor Rectifier with Improved Dynamic Response for Non-linear Load

D.V. Nicolae

Abstract: *In this paper, a robust controller asserting a unity power factor rectifier is studied. The inner current control loop is a hysteresis type with switching frequency kept below a maximum imposed value; the harmonics generated are spread in certain range below the maximum imposed frequency and thus reducing the electromagnetic interference. The voltage controller feed-forwards the information about the dc output power to improve the dynamic response for any type of dc load. To demonstrate the improved response of the voltage regulator, a buck regulator as non-linear load drawing approximately 2.5 kW, is used.*

Key Words*: Harmonics, Hysteresis Current Controller, Feedforward Voltage Controller, Power Factor Correction*

Nomenclature

$v_s(t)$ – supply voltage
$\hat{V}_s$ – supply voltage amplitude
V_s – supply rms voltage
f_s – supply frequency
$i_s(t)$ – supply current
$\hat{I}_s$ – supply current amplitude
I_s – supply rms current
$i_s^*(t)$ – reference supply current
I_s^* - amplitude of the supply reference current
R_s, L_s – elements of source impedance
R_F, L_F – elements of input inductance
v_c – input converter voltage
C – capacitor; dc storage element
V_o – output dc bus voltage
V_o^* – reference output dc bus voltage
I_o – output dc current
P_o – output dc power
R_L – output dc load
$SC_{1,2,3,4}$ – signal conditioners
$\tau_{1,2,3,4}$ – time constants
ξ – dumping coefficient
$F_p(s)$ – plant transfer function referred to the current controller
$F_c(s)$ – compensator transfer function referred to the current controller
$F_{lf}(s)$ – low-pass filter transfer function referred to the current controller
f_o – maximum imposed switching frequency for the current controller
f_{osc} – actual switching frequency for the current controller
K_c – current controller compensator gain
k_i – integral coefficient
k_p – proportional coefficient

I. Introduction

The AC to DC converter is usually the first stage for most of the electronic equipments. In the early years, this function has been performed by a diode bridge rectifier coupled with a capacitive smoothing filter. This solution generates high level of harmonics in the supply current. Standard bodies have issued limits to the harmonics pollution such as IEC 1000-3-2 and EN 60555-2 [1], [2].

Single-phase power factor rectifiers (UPFR) are used more and more to supply small to medium power loads. The topic has been extendedly covered with various topologies [2] … [6] and control systems [7] … [13]. Many authors used as current controller techniques such as PWM [8], non-linear carrier [11], bang-bang with predicted switching frequency [7]. As a general conclusion, these controllers use either a fixed carrier PWM modulation or hysteresis. The inconvenient of a fixed carrier is the concentration of entire switching energy in only one spectral frequency and this could create interference problems. Generally, the hysteresis method generates high switching frequencies which produce high stress on switching devices.

The focus in this paper is on a simple and performing current and voltage controller. The current controller proposed in this paper is basically a hysteresis one but the introduced modification imposed a limit to the highest switching frequency and the switching spectral lines are spread on a relatively wide range and thus significantly reducing the interferences.

Manuscript received January 2007, revised January 2007

The proposed voltage controller introduces output power estimation in order to improve the load dynamic response.

II. System Configuration

The proposed system is presented in Fig. 1. The central component of the system is a full bridge switching mode converter built with MOSFET and designed to operate safe up to 2.5 kW. The connection with the ac supply network is realized via the inductance Z_F (L_F, R_F). The condenser C represents the dc bus storage element.

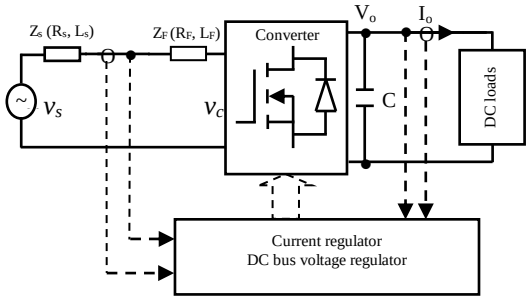

Fig. 1 System configuration

When the dc load draws current, the input current is shaped by the current controller to be sinusoidal and in phase with the voltage. As input parameters for the control system, a minimal solution has been used: supply current, supply voltage, dc bus voltage and current.

III. Control System

III.1. Current Controller

As mentioned before, the current controller proposed in this study is of hysteresis type with an imposed upper limit for the switching frequency. The block diagram of this controller is shown in Fig. 2, where Cv represents the switching-mode converter, SC_1 and SC_2 the signal conditioners which convert the current and voltage parameters into proper signals, F_p (s) the plant transfer function, F_c (s) the compensator transfer function and F_{lf} (s) the transfer function of the upper limiter of the switching frequency. The phase-lock loop (PLL) extracts the frequency (wt) creates the reference current $i_s^*(t)$ using the reference amplitude I_s^* coming from the voltage regulator.

Let's firstly consider the system without compensator. The plant is the input resistor and its transfer function is:

$$F_p(s) = 1/(R_F + L_F \times s) \tag{1}$$

This transfer function introduces a phase shift of -900. Basically, the principle of hysteresis is an oscillation around a set value. In order to have an 180^0 phase shift, a low-pass filter has been introduced F_{lf} (s).

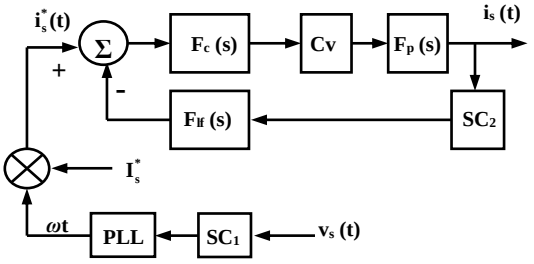

Fig. 2 Current controller

The choice of this was a second order Butterworth filter (dumping factor $\xi = 0.707$) which does not affect the operating frequency. At the switching frequency it introduces a phase rotation of nearly -90^0. Due to the delay group time produced, the final result is controlled limitation of the highest switching frequency (ω_o).

$$F_{lf}(s) = 1/\left[1 + 2(\xi/\omega_o) \times s + s^2/\omega_o^2\right] \tag{2}$$

Thus the closed loop transfer function becomes:

$$H(s) = \frac{1}{1 + \left(\frac{L_F}{R_F} + \frac{2\xi}{\omega_o}\right)s + \left(\frac{2\xi L_F}{R_F \omega_o} + \frac{1}{\omega_o^2}\right)s^2 + \left(\frac{L}{R_F \omega_o^2}\right)s^3} \tag{3}$$

Study of this third order system shows good stability. The relation between the oscillation frequency and the maximum imposed is given as:

$$f_{osc} / f_o = \sqrt{1 + 2 \times \xi \times R_F / (\omega_o \times L_F)} \tag{4}$$

The compensator F_c (s) is introduced to improve the static error and the system bandwidth. The compensator chosen for this study is:

$$F_c(s) = K_c \cdot \frac{1 + \tau_2 \cdot s}{1 + \tau_1 \cdot s} \tag{5}$$

where:

$$K_c = \tau_1/\tau_2 \tag{6}$$

This compensator acts as a PI controller for medium to high frequencies and for low frequencies increases the open loop gain by K_c and thereby reducing the static error. For this reason, it has been chosen $\tau_1 < \tau_2$: low

frequency gain higher than one. For this study, the following values have been chosen:

$$\tau_1 = 1/ (2\times\pi\times25) \quad (7)$$

$$\tau_2 = 1/ (2\times\pi\times500) \quad (8)$$

$$\omega_o = 1/ (2\times\pi\times10^4) \quad (9)$$

Then the stability of this controller has been studied using Matlab simulation platform. Fig. 3 shows the root-locus and open-loop Bode diagram.

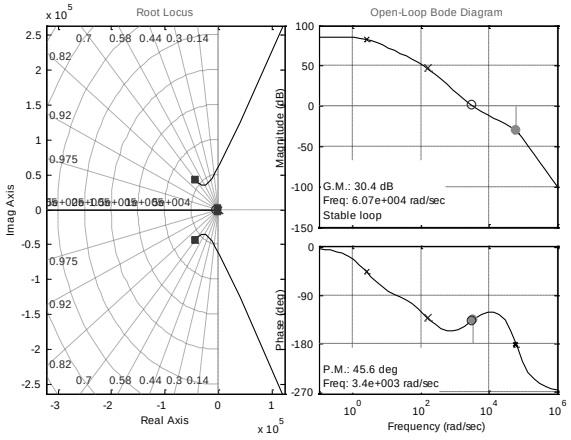

Fig. 3 Current controller: root locus and Bode diagram

III.1. Voltage Controller

In the steady-state, when the input current is sinusoidal shaped, the equation system which governs the single-phase UPFR can be written as:

$$v_s(t) = \left(R_s + R_F\right) i_s + \left(L_s + L_F\right)\frac{di_s}{dt} + v_c \quad (10)$$

$$\Delta I_s = \frac{V_o}{4 f_c L_F} \quad (11)$$

$$2\hat{V}_s\hat{I}_s = \frac{1}{C}\cdot\frac{d}{dt}\left(V_o^2\right) + V_o I_o \quad (12)$$

$$V_o \geq \sqrt{V_s^2 + I_s^2\left[\left(R_s + R_F\right)^2 + (\omega_s L_F)^2\right]} \quad (13)$$

where v_s, i_s are the supply voltage and current, ΔI_s is the ripple at the input current, v_c is the input voltage of the active converter and V_o and I_o are the dc output parameters. The dc voltage V_o should comply with the controllability criteria (13).

Majority of authors use as regulator a PI solution. But the closed-loop transfer function of this type of regulator has two zeros [14]:

$$\frac{V_o^2}{V_o^{*2}} = \frac{\left(k_i + s\times k_p\right)\left(1 + s\times\tau_3\right)}{s^3\times\left(\frac{\tau_3 C}{2}\right) + s^2\times\frac{C}{2} + s\times k_p + k_i} \quad (14)$$

For this study an integral/proportional (Fig. 4) solution has been chosen as voltage regulator.

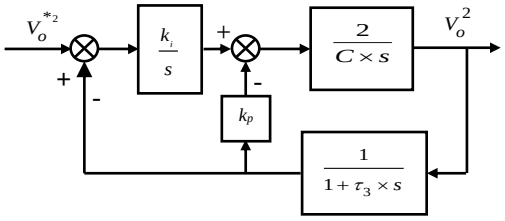

Fig. 4 IP voltage regulator

The close-loop transfer function of the system is:

$$\frac{V_o^2}{V_o^{*2}} = \frac{1 + s\times\tau_3}{s^3\left(\frac{\tau_3\times C}{2k_i}\right) + s^2\left(\frac{C}{2k_i}\right) + s\left(\frac{k_p}{k_i}\right) + 1} \quad (15)$$

The equation (15) shows that the IP solution cancels a slow zero from the transfer function improving the dynamics of the regulator.

If the poles of the system (s_0, s_1 and s_2) are placed on the Butterworth circle with the radius ω_o such as: $s_o = -\omega_o$, $s_1 = \omega_o e^{j\frac{3\pi}{4}}$ and $s_2 = \omega_o e^{-j\frac{3\pi}{4}}$, then the coefficients k_p and k_i are:

$$k_p = \frac{C}{2\times\left(1+\sqrt{2}\right)\times\tau_3} \quad (16)$$

$$k_i = \frac{C}{2\times\left(1+\sqrt{2}\right)^3\times\tau_3^2} \quad (17)$$

But, according to (12), one should also consider the dc power delivered to the dc load. If an equivalent resistance R_L parallel to the capacitor C substitutes the dc load, then using the same procedure as for equations (16) to (17) the new coefficients of the IP regulator can be written:

$$k_i' = \frac{\left(T+\tau_3\right)^3}{T^2\tau_3^2\left(1+\sqrt{2}\right)^3 R_L} \quad (18)$$

$$k_p' = \frac{1}{R_L}\left(\frac{\left(T+\tau_3\right)^2}{\left(1+\sqrt{2}\right)T\tau_3} - 1\right) \quad (19)$$

where $T = R_L \times C$ and τ_3 is the constant of the low-pass filter.

Since the main function is to force the input current to have a sinusoidal shape related to the line frequency, then the low pass filter cut-off frequency of the voltage regulator is recommended to be between 0.33 and 0.5 from the line frequency [14].

The important aspect noticed for this approach is that the regulator coefficients should be corrected every time when the dc load is changed. In order to address this drawback, a dc power estimator (using the dc bus voltage and current via a signal conditioners SC_3 and SC_4) working as feed-forward is introduced in the diagram of the voltage regulator (Fig. 5) used in this study. The principle of feed-forward was studied in [15] but only using current information. Using this configuration, the proportional and integral coefficients will be again given by (16) and (17).

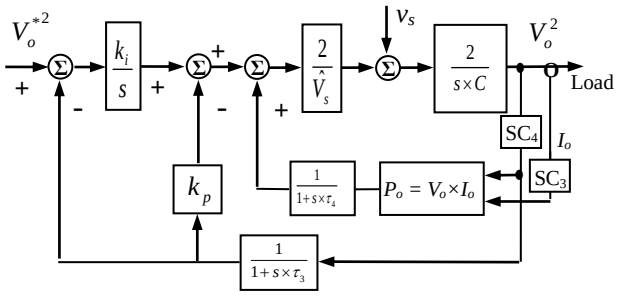

Fig. 5 Block diagram for the proposed voltage regulator

The time constant τ_4 does not affect the performances of the voltage regulator; this low pass filter is used to reject high frequency noise.

A large value of the capacitor C can reduce the ripple of the dc bus, but also reduces the dynamic of the regulator.

Further, Fig. 6 shows the Nyquist stability of the voltage regulator.

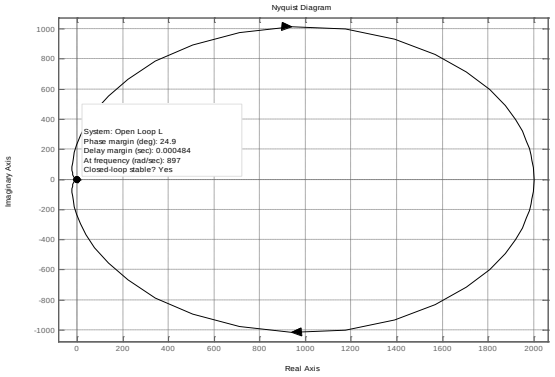

Fig. 6 Voltage regulator: Nyquist stability

IV. Simulation results

Using Matlab simulation software, the performances of the proposed converter have been studied. As mention before a compromise between the ripple and dynamic of the voltage regulator should be considered hence a value of C = 1000μF has been chosen. With this value the proportional and integral coefficients become: $k_p = 0.02589$ and $k_i = 0.5552$.

The other parameters of the platform are $V_s = 220$ V_{rms} /50Hz, $R_s = 1m\Omega$, $R_F = 50m\Omega$, $L_s = 0.1mH$ and $L_F = 10mH$, $V_o = 500$ V and $P_o = 2.5$ kW.

IV.1. Steady State

Fig. 7 shows the parameters of the unity power factor ac to dc converter under steady state conditions.

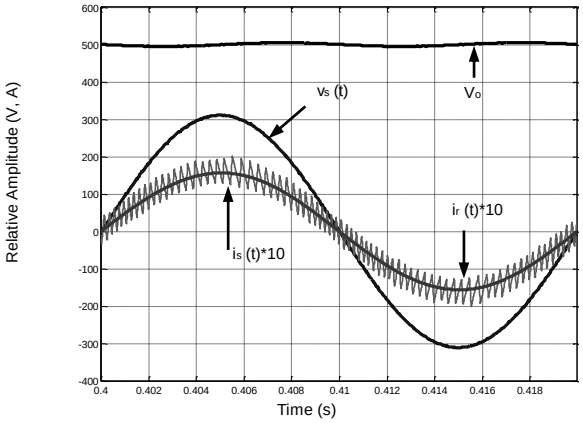

Fig. 7 Steady state parameters

From the above figure it is possible to notice the input current follows perfectly the reference one and is in phase with the supply voltage. It can also be noticed, the dc voltage follows the imposed reference of 500 V.

Fig. 8.a shows the supply current spectrum for normal industrial range. It can be noticed a very good total harmonic distortion of 1.6 percentage.

Fig. 8b shows an expanded spectrum of the input current. It can be seen that the switching frequency does not introduces only one strong spectral line but a multitude of low amplitude lines with lower frequencies than the imposed maximum of 10 kHz. This validates the property of the proposed current controller.

IV.2. Impact of the Dc Load Step

The next step was to study the dynamic behavior for a step variation of the dc load. Fig. 9 shows the dynamic of the system for a step down and up for the system with and without power estimator in the voltage regulator.

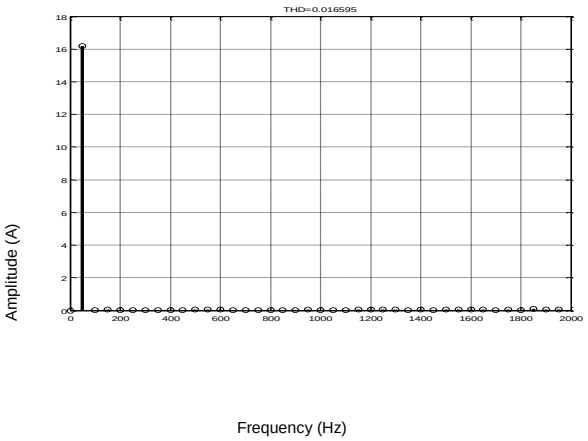

(a)

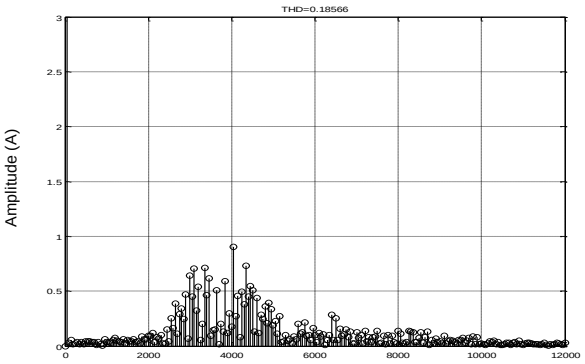

(b)

Fig. 8 Input current: spectrum

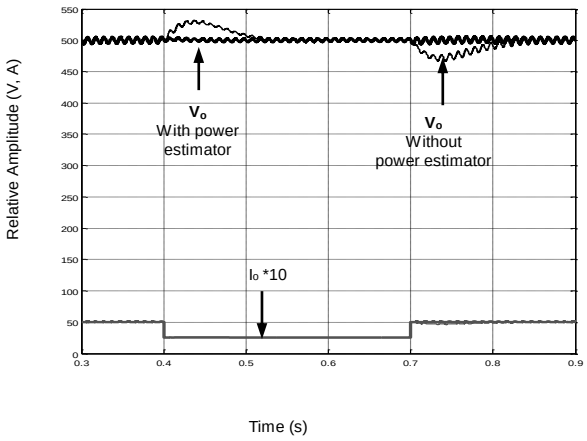

Fig. 9 Dynamic response for step down/up of dc load

As can be noticed, the over shoot and under shoot for the voltage regulator with power estimator is practically none compared with the situation where this block is not introduced.

IV.3. Influence of a non-linear dc load

For further investigation, a "non-linear" dc load has been introduced in order to study the dynamic response. Such a load was a pulsating dc current drawn by a buck regulator with a switching frequency of 1 kHz acting as battery charger or dc motor drive. Fig. 10 shows the response of proposed voltage regulator for a step down in the "non-linear" dc load and Fig. 11 for a step up.

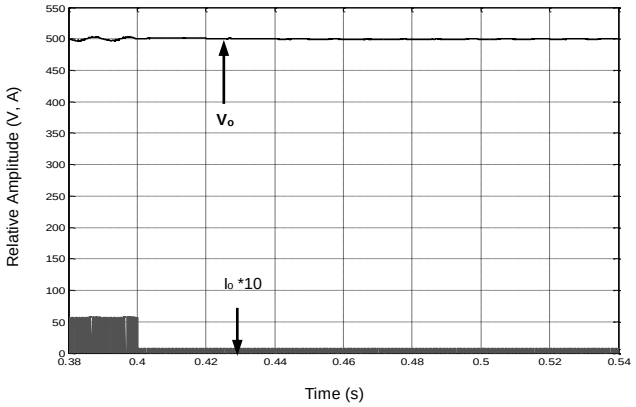

Fig. 10 Dynamic response for a step down of a nonlinear load

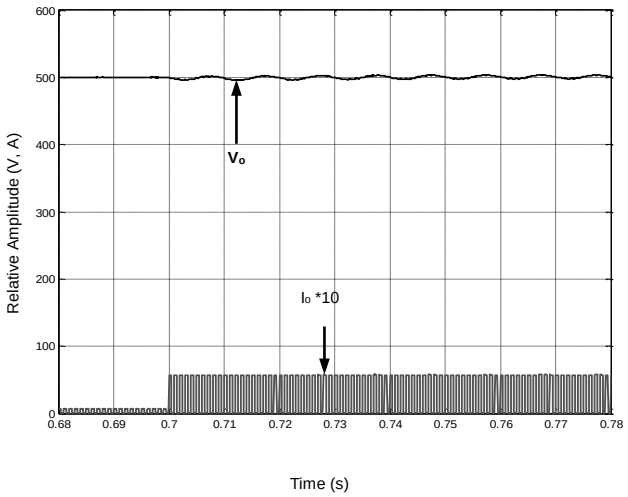

Fig. 11 Dynamic response for a step up of a nonlinear load

As can be noticed from the above figures (10 & 11), response of the system is very good with no over and under shoot; the only change is in ripple which is normal.

V. Experimental results

To validate the proposed controller and to verify the simulation results, an experimental model (see Fig. 12) based on fast IGBT has been built using the same input and output parameters and C =1000 μF. The signal conditioners ratio which have been: 10 A to 1V for the currents and 1000 V to 1 V for the voltages. Thus, the

adjusted proportional and integral coefficients became: $k_p = 2.589\times10^{-8}$ and $k_i = 55.52\times10^{-8}$.

During the experiments, the supply voltage has been used to provide the information about its amplitude and frequency; an automatic gain control amplifier converted the supply voltage into a unity amplitude signal which has been further used to crate the current reference. In this way the entire UPFR could be seen as a "linear load", the current being in phase and having the same shape as supply voltage.

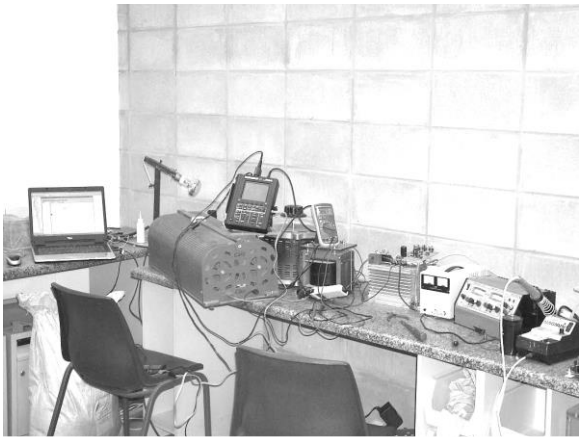

Fig. 12 Experimental model setup

The parameters monitored during the experiments have been the input current and dc bus voltage. Fig. 13 shows the input current versus reference current for full output dc load. It can be seen, the input current follows very well the reference. The ripple is a little bit high due to the input inductance which in this situation is 7.2 mH. In Fig. 14 it is observed the highest switching frequency which can be estimated as 6-7 kHz.

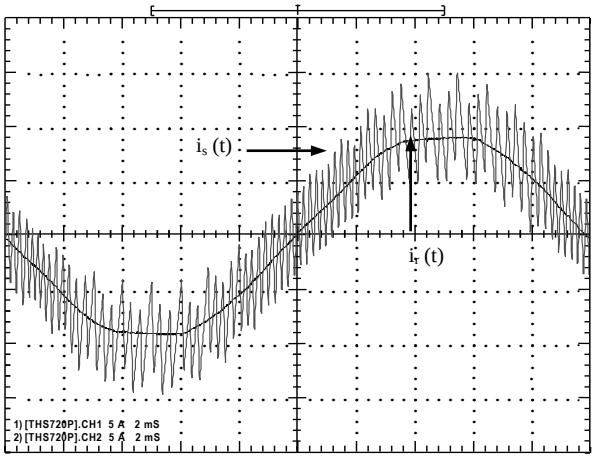

Fig. 13 Reference and supply current

From Fig. 15 it can be observed that the input voltage and input current are in phase and the current follows the shape of the voltage.

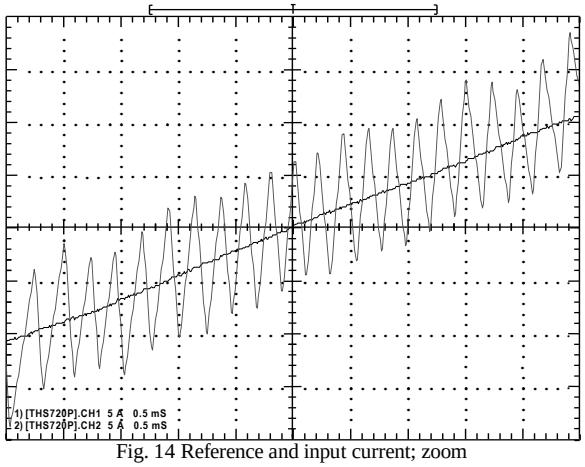

Fig. 14 Reference and input current; zoom

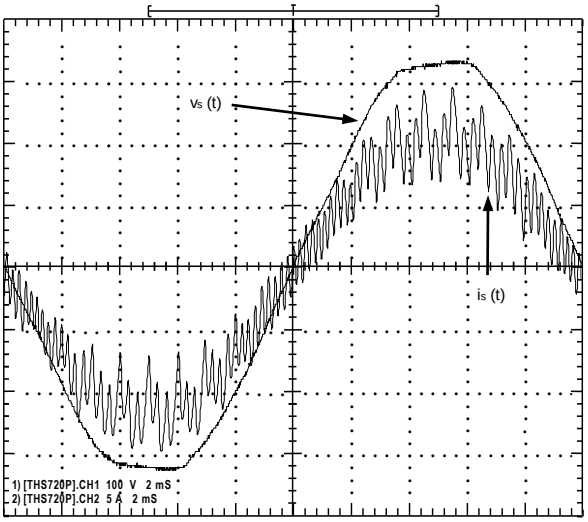

Fig. 15 Input voltage and current

Fig. 16 shows the response of the system for a sudden decrease of the "pulsating dc current" from 5.6 A to 0.5 A, while Fig. 16 shows the reverse step up of the current.

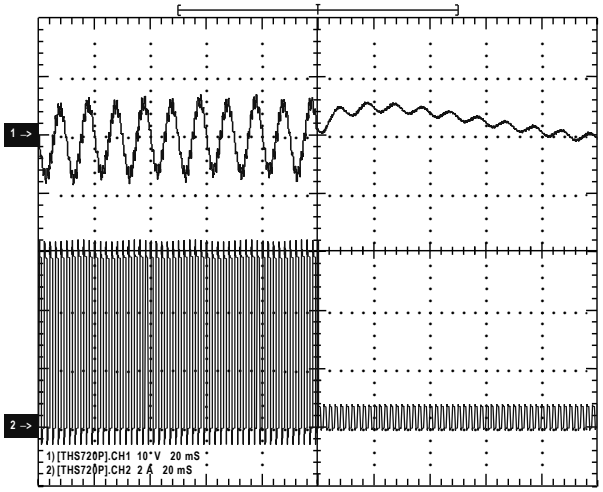

Fig. 16 Impact of step down in dc load

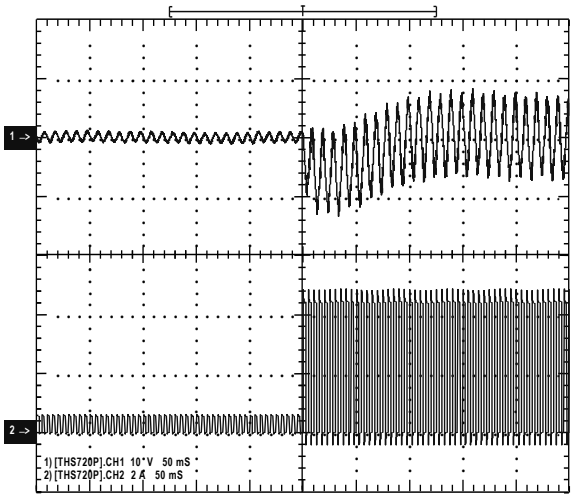

Fig. 16 Impact of step down in dc load

It can be noticed, the dc voltage (here is "ac coupled" for better view) has a very small variation and the settling time is about 0.1 seconds.

VI. Conclusion

This paper presented the concept and behavior of a unity power factor rectifier with a control system which ensure a very good dynamic response for linear and "non-linear" dc loads.

The simulation and experimental results on a 2.5 kW model validate the concept: the switching frequency is kept below the imposed maximum value and the dynamic response shows small under and over shoot with a settling time of approximately 0.1 seconds.

References

[1] H. Mao, F.C. Lee, Y. Jiang and D. Borojevic, Review of Power Factor correction techniques, 2nd IPEMC 1997, pp. 9-21

[2] Ch. Andrieu, J.P. Ferrieux and M Rocher, The ac/dc stage: A survey of the structures and chopper control modes for power factor correction, EPE Journal, Vol. 5, No3/4, pp. 17-22, Jan. 1996

[3] M.H.L. Chow & all, A Novel Method for Elimination of Line - Current Harmonics in Single-Stage PFC Switching Regulators, IEEE Transactions On Power Electronics, Vol.13, No. 1, January 1998

[4] C. Qiao & all, An Improved Integration-Reset Controlled Single-Phase Unity- Power-Factor Boost Rectifier with Lower Distortions, IECON 1999

[5] J. Qian, F.C. Lee, Charge Pump Power-Factor-Correction Technologies; Part I: Concept and Principles, IEEE Transactions on Power Electronics, Vol.15, No. 1, January 2000

[6] J. Qian, Q. Zhao, F.C. Lee, Single-Stage Single-Switch Power-Factor-Correction AC/DC Converter with DC-Bus Voltage Feedback for Universal Line Applications, IEEE Transactions on Power Electronics, Vol.13, No. 6, November 1998

[7] M. Dawande, G.K. Dubey, Bang-Bang Current Control with Predecided Switching Frequency for Switch-Mode Rectifiers, IEEE Transactions on Industrial Electronics, Vol. 46, No. 1, February 1999

[8] S. Ben-Yaakov, I. Zeltser, The Dynamics of PWM Boost Converter with Resistive Input, PESC 1998, pg. 885-890

[9] G. Ioanidis, A. Kanadianis, S.N. Manias, Novel Control Design for the Buck Converter, IEE Proc.-Electr. Power Appl., Vol. 145, No. 1, Jan. 1998

[11] R. Zane, D. Maksimovič, Nonlinear-Carrier Control for High-Power-Factor Rectifiers Based on Up-Down Switching Converters, IEEE Transactions On Power Electronics, Vol. 13, No. 2, March 1998

[12] M.O. Eissa & all, Fast Controller for a Unity-Power Factor PWM Rectifier, *IEEE Transactions On Power Electronics*, Vol. 11, No.1, Jan. 1996

[13] A.S. Martins, E.V. Kassick, I. Barbi, Control Strategy for the Double Boost Converter in Continuous Conduction Mode Applied to Power Factor Correction, *PESC 1996*, pg. 1066-1072

[14] N. Bruyant, M. Machmoum, P. Chevrel "Control of a three-phase active power filter with optimized design of the energy storage capacitor", *PESC 98*, pp. 878-883

[15] M.-T. Tsai, W.I. Tsai, Analysis and Design of Three-Phase AC-to-DC Converters with High Power Factor and Near-Optimum Feedforward, *IEEE Trans. On Ind. Electronics*, Vol.46, No.3, June 1999, pp 535-543

Author's information

Department of Electrical Engineering
Tshwane University of Technology
Private Bag X07, 0116 Pretoria North,
South Africa

Dan Valentin Nicolae (M) was born in 1948, in Bucharest, Romania. He graduated the Polytechnic University of Bucharest, Romania in July 1971 with MSc degree and got his doctorate degree in 2004 at Vaal University of Technology, South Africa.

After graduation he worked as researcher in the Institute for Nuclear Technologies, National Institute for Scientific and Technological Creativity - Avionics Division, Bucharest, Romania. In 1998 he joined Electrical Department Tshwane University of Technology, South Africa.

He is doing research in the field of power converters, control of electric machines and non-conventional power extraction from high voltage transmission lines.

Dr. Nicolae is a member of IEEE, Engineering Counsel of South Africa and South African Institute of Electrical Engineers.